JOURNAL OF BACTERIOLOGY, June 1997, p. 3458–3469 Vol. 179, No. 11
0021-9193/97/$04.00+0

Maximization of Transcription of the *serC* (*pdxF*)-*aroA* Multifunctional Operon by Antagonistic Effects of the Cyclic AMP (cAMP) Receptor Protein-cAMP Complex and Lrp Global Regulators of *Escherichia coli* K-12

TSZ-KWONG MAN, ANDREW J. PEASE, AND MALCOLM E. WINKLER*

Department of Microbiology and Molecular Genetics, University of Texas Houston Medical School, Houston, Texas 77030-1501

Received 13 February 1997/Accepted 25 March 1997

The arrangement of the *Escherichia coli serC* (*pdxF*) and *aroA* genes into a cotranscribed multifunctional operon allows coregulation of two enzymes required for the biosynthesis of L-serine, pyridoxal 5′-phosphate, chorismate, and the aromatic amino acids and vitamins. RNase T_2 protection assays revealed two major transcripts that were initiated from a promoter upstream from *serC* (*pdxF*). Between 80 to 90% of *serC* (*pdxF*) transcripts were present in single-gene mRNA molecules that likely arose by Rho-independent termination between *serC* (*pdxF*) and *aroA*. *serC* (*pdxF*)-*aroA* cotranscripts terminated at another Rho-independent terminator near the end of *aroA*. We studied operon regulation by determining differential rates of β-galactosidase synthesis in a merodiploid strain carrying a single-copy λ{Φ(*serC* [*pdxF*]′-*lacZYA*)} operon fusion. *serC* (*pdxF*) transcription was greatest in bacteria growing in minimal salts-glucose medium (MMGlu) and was reduced in minimal salts-glycerol medium, enriched MMGlu, and LB medium. *serC* (*pdxF*) transcription was increased in *cya* or *crp* mutants compared to their cya^+ crp^+ parent in MMGlu or LB medium. In contrast, *serC* (*pdxF*) transcription decreased in an *lrp* mutant compared to its lrp^+ parent in MMGlu. Conclusions obtained by using the operon fusion were corroborated by quantitative Western immunoblotting of SerC (PdxF), which was present at around 1,800 dimers per cell in bacteria growing in MMGlu. RNase T_2 protection assays of *serC* (*pdxF*)-terminated and *serC* (*pdxF*)-*aroA* cotranscript amounts supported the conclusion that the operon was regulated at the transcription level under the conditions tested. Results with a series of deletions upstream of the $P_{serC\ (pdxF)}$ promoter revealed that activation by Lrp was likely direct, whereas repression by the cyclic AMP (cAMP) receptor protein-cAMP complex (CRP-cAMP) was likely indirect, possibly via a repressor whose amount or activity was stimulated by CRP-cAMP.

The transaminase encoded by the *serC* (*pdxF*) gene of *Escherichia coli* (EC 2.6.1.52) catalyzes the second and third steps in the serine and pyridoxal 5′-phosphate (PLP) biosynthetic pathways, respectively (Fig. 1). In the serine pathway, SerC (PdxF) adds an amino group to the three-carbon precursor, 3-phosphohydroxypyruvate, to form 3-phosphoserine, which is dephosphorylated by the SerB phosphatase to form serine (58). In the PLP pathway, SerC (PdxF) adds an amino group to the four-carbon precursor 3-hydroxy 4-phosphohydroxy α-ketobutyrate to form 4-phosphohydroxy-L-threonine (13, 24, 31, 36), which provides the nitrogen group and phosphoester groups of pyridoxine 5′-phosphate (PNP) and PLP (23, 24, 65, 68). Because *serA*-encoded 3-phosphoglycerate dehydrogenase greatly favors its reverse (reductase) reaction (49, 61, 62, 71), the SerC (PdxF) transaminase pulls serine biosynthesis in the forward direction and likely contributes to the control of the flux of intermediates through the pathway (61, 67, 71). SerC (PdxF) may play a similar crucial role in setting the rate of PLP biosynthesis, although sustained 4-phosphoerythronate dehydrogenase or 3-hydroxy 4-phosphohydroxy α-ketobutyrate reductase activity has not yet been attained in vitro (67). The SerC (PdxF) transaminase itself requires PLP as a coenzyme (8, 10, 13), and sufficient PLP must be synthesized to sustain SerC (PdxF) function in both PLP and serine biosynthesis.

DNA sequence and genetic polarity analyses established that the *E. coli* K-12 *serC* (*pdxF*) gene is upstream from *aroA* in a multifunctional operon that contains at least these two genes (14, 25, 31). *aroA* encodes enolpyruvolylshikimate 3-phosphate synthase, which catalyzes the penultimate step in the common aromatic pathway leading to chorismate (48). *aroA* mutants of a variety of pathogenic bacteria are avirulent and have been used extensively in the production of vaccines (12, 60). The cotranscription of *serC* (*pdxF*) and *aroA* is conserved in several bacterial species besides *E. coli*, including *Salmonella typhimurium* and *S. gallinarum* (21, 25) and *Yersinia enterocolitica* (46). Although it is possible that this conserved grouping is accidental, it probably reflects the need to coordinately regulate the biosynthesis of serine, PLP, and chorismate in some kinds of bacteria (15, 31, 48). PLP and chorismate biosynthesis are linked by the utilization of erythrose 4-phosphate as the starting compound in each pathway (Fig. 1) (31, 48, 67, 69), and chorismate and serine are required in equimolar amounts for the biosynthesis of the iron chelator enterochelin (14, 48). Moreover, PLP, serine, and aromatic compounds are linked in numerous steps and branches of intermediary metabolism. For example, chorismate is the precursor of tetrahydrofolate (20), which captures one-carbon units when serine is cleaved to glycine by PLP-dependent serine hydroxymethyltransferase (38, 58).

Despite the important roles of the SerC (PdxF) transami-

* Corresponding author. Mailing address: Department of Microbiology and Molecular Genetics, University of Texas Houston Medical School, 6431 Fannin, JFB 1.765, Houston, TX 77030-1501. Phone: (713) 500-5461. Fax: (713) 500-5499. E-mail: mwinkler@utmmg.med.uth.tmc.edu.

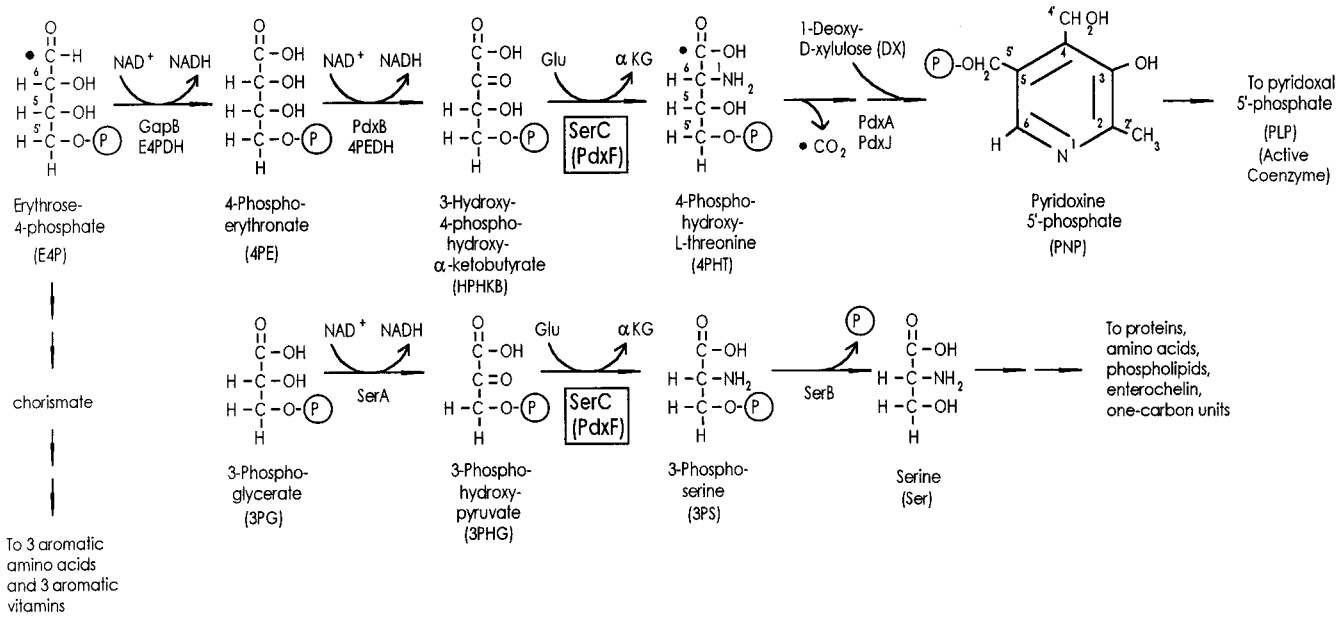

FIG. 1. Dual function of the SerC (PdxF) transaminase in the biosynthesis of serine and the B_6 vitamers PNP and PLP in *E. coli* K-12. Evidence for the parallel pathways of 3-phosphoserine and 4-phosphohydroxy-L-threonine biosynthesis and the involvement of the SerC (PdxF) transaminase in both pathways is summarized in the introduction. SerA, 3-phosphoglycerate dehydrogenase; SerB, 3-phosphoserine phosphatase; GapB, erythrose 4′-phosphate dehydrogenase (E4PDH); PdxB, 4-phosphoerythronate dehydrogenase (4PEDH). PdxA and PdxJ are thought to be involved in formation of the PNP pyridine ring from 1-deoxy-D-xylulose and 4-phosphohydroxy-L-threonine (23, 24, 30, 31, 36, 68).

nase and AroA synthase in intermediary metabolism, relatively little is known about the transcriptional organization and regulation of the *serC* (*pdxF*)-*aroA* operon (58). In the first structural study of this operon, Duncan and Coggins identified a likely $P_{serC\ (pdxF)}$ promoter from transcripts synthesized from a multicopy recombinant plasmid (Fig. 2) (14). The promoter contained an extended 26-bp region of dyad symmetry overlapping the −10 box (14), and a putative cyclic AMP (cAMP) receptor protein-cAMP complex (CRP-cAMP) binding site was located 57 bp upstream from the −35 box (Fig. 2) (34). DNA sequence analyses suggested that Rho factor-independent transcription terminators were located between *serC* (*pdxF*) and *aroA* and after *aroA* (Fig. 2) (14, 31). Unpublished preliminary Northern and S1 mapping analyses suggested that the terminator between *serC* (*pdxF*) and *aroA* functioned as an attenuator of *aroA* transcription to some unspecified degree, and the terminator after *aroA* ended the operon (15).

Early experiments suggested that *serC* (*pdxF*) expression might be reduced by combinations of amino acids (39, 50), but the assay for SerC (PdxF) transaminase activity was indirect in these studies. AroA synthase specific activity was reduced significantly in cells grown in a medium containing all 20 amino acids, but *aroA* expression was considered constitutive with respect to repression by aromatic amino acids and the TyrR and TrpR repressors (18, 48, 63). Recently, it was reported that *serC* (*pdxF*)-*aroA* operon expression was induced about twofold by CRP-cAMP (34); however, no explanation was given for the physiological significance of this induction. Here, we confirm that the *serC* (*pdxF*)-*aroA* operon consists of only two genes and show that the *aroA* transcript amount is five- to eightfold lower than that of *serC* (*pdxF*), possibly through the action of an attenuator between *serC* (*pdxF*) and *aroA*. We also show that the *serC* (*pdxF*)-*aroA* operon is in fact repressed by CRP-cAMP and activated by the leucine-responsive protein (Lrp) at the transcriptional level. The combined effect of these two global regulators is to maximize *serC* (*pdxF*)-*aroA* operon expression in cells growing in minimal salts medium with glucose as the carbon source.

MATERIALS AND METHODS

Materials. Sodium *N*-lauroylsarcosine, goat anti-rabbit immunoglobulin G antibody (whole molecule) conjugated with alkaline phosphatase, and other biochemicals were from Sigma Chemical Co. (St. Louis, Mo.). Vitamin assay Casamino Acids and Bacto Agar were from Difco Laboratories (Detroit, Mich.). LB medium and agar capsules (10 g of NaCl per liter) were purchased from Bio 101 (Vista, Calif.). Some restriction endonucleases, Vent (Exo^+) and Vent (Exo^-) DNA polymerases, and 10× PCR buffer were from New England Biolabs (Beverly, Mass.). Other restriction endonucleases, T4 DNA polymerase, T7 RNA polymerase, riboprobe Gemini system II, RQ1 DNase, plasmid pGEM-3Z, deoxynucleoside triphosphate mixtures, nitroblue tetrazolium, and 5-bromo-4-chloro-3-indolylphosphate were bought from Promega, Inc. (Madison, Wis.). RNase T_2 and custom DNA oligomers were purchased from Gibco-BRL (Gaithersburg, Md.). [α-^{32}P]CTP (10 mCi per ml; >400 Ci per mmol) was purchased from Amersham Corp. (Arlington Heights, Ill.). Polyvinylidene difluoride membranes (0.2 μm) were from Pierce Chemical Co. (Rockford, Ill.). Polyhistidine (His_6)-tagged SerC (PdxF) was purified as described before (16) and used as an antigen to produce anti-SerC (PdxF) polyclonal antibodies in rabbits (70). Native SerC (PdxF) was the gift of Genshi Zhao (66).

Culture media. Minimal salts Vogel-Bonner (1× E) medium containing 0.01 mM $FeSO_4$ was prepared as described previously (7). MMGlu was 1× E medium containing 0.4% (wt/vol) glucose. Enriched MMGlu (EMMGlu) was MMGlu supplemented with 0.5% (wt/vol) vitamin assay Casamino Acids. MMGly was 1× E medium containing 1% (vol/vol) glycerol. The concentration of 5-bromo-4-chloro-3-indolyl-β-D-galactopyranoside (X-Gal) in LB agar plates was 40 μg per ml. Antibiotics were added to LB at the following concentrations: 50 μg of kanamycin per ml, 50 μg of ampicillin per ml, 25 μg of chloramphenicol per ml, 50 μg of streptomycin per ml, and 50 μg of tetracycline per ml. Half of the concentration of antibiotics except tetracycline was added to minimal media. Overnight starter cultures containing appropriate antibiotics were inoculated from frozen permanent stocks and grown in the same media to be used in final experiments. Overnight cultures (0.5 to 1%, vol/vol) were inoculated into sidearm flasks containing final media lacking antibiotics. Flasks were grown with vigorous shaking (≈300 rpm) at 37°C.

Bacterial strains and plasmids. Bacterial strains and plasmids used in this study are listed in Table 1. Bacteriophage P1*vir*-mediated generalized transduction and preparation of bacteriophage λ lysates were carried out as described previously (41, 55). Recombinant plasmids were constructed by standard tech-

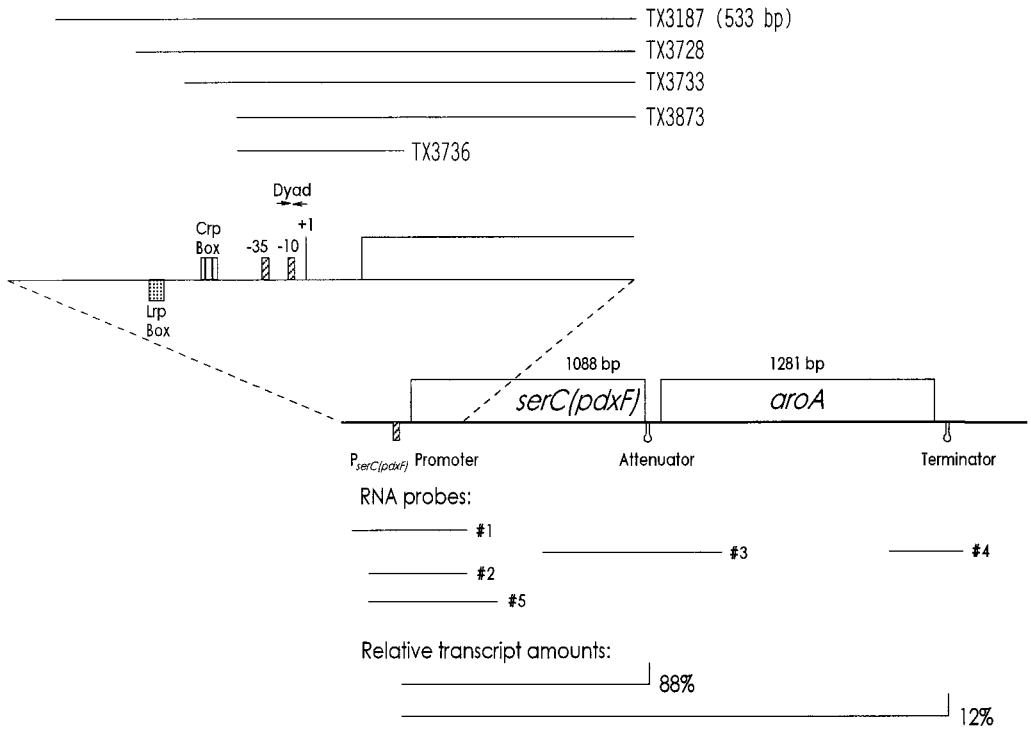

FIG. 2. Organization and transcriptional patterns of the *serC* (*pdxF*)-*aroA* multifunctional operon at 20.58 min on the *E. coli* K-12 chromosome (28). The *serC* (*pdxF*) and *aroA* reading frames are indicated by boxes drawn to scale. The positions of likely Rho-independent terminators in the *serC* (*pdxF*)-*aroA* intercistronic space and downstream from *aroA* are marked (see text). The enlarged diagram of the $P_{serC\ (pdxF)}$ promoter region shows the Lrp and CRP boxes analyzed here (see text). The position in the $P_{serC\ (pdxF)}$ −10 region of a strong dyad symmetry reminiscent of an operator is indicated (14, 15, 31). The lines at the top show the segments contained in the indicated λ{Φ(*serC* [*pdxF*]′-*lacZ*)} operon fusion strains (Table 1). The lines at the middle show the RNA probes used in RNase T_2 protection assays. The relative amounts of *serC* (*pdxF*) single-gene and *serC* (*pdxF*)-*aroA* cotranscript are shown at the bottom. See Results for details.

niques (54). Restriction fragments were purified from agarose gels by the Wizard PCR DNA purification system, and plasmid DNA was purified by the Wizard Miniprep DNA purification system (Promega).

Φ(*serC* [*pdxF*]′-*lacZYA*) operon fusions were constructed in plasmid vector pRS551 (Table 1) (56). Initial ligation mixtures were transformed into *E. coli* DH5α (*recA*), and plasmids from putative clones were screened by digestion with appropriate restriction enzymes. Fusion junctions of deletion-containing plasmids pTX509, pTX510, and pTX511, which were used to construct pTX518, pTX519, and pTX520, respectively, were verified by automatic DNA sequencing using EXT7-1 and SP6-1 primers by the DNA core facility in this department. As expected from the cloning scheme, pTX509, pTX510, pTX518, and pTX519 contained 10 extra nucleotides (nt) from the polycloning site of pGEM-3Z at the 3′ end of the fusion junction compared to pTX520 and pTX552. Correct plasmids were transformed into strain S90C (*recA*$^+$), which was lytically infected with phage λRS88 (*imm*^{434} *c*I^{ind}) as described before (56). Final lysogens were formed in strain NK7049 (Δ*lac*) (56) and selected on LB–X-Gal or MacConkey-lactose (1%, wt/vol) plates containing streptomycin and kanamycin. Putative lysogens were screened for sensitivity to ampicillin to eliminate carryover of intact plasmids, and single-copy prophage were identified by 3-primer PCR (below).

Transcript mapping by RNase T_2 protection assays. Fifteen-milliliter cultures in the media indicated were grown at 37°C to a turbidity of 50 Klett (660 nm) units (≈3.3×10^8 cells per ml in MMGlu and 2.8×10^8 cells per ml in LB). RNA was purified by adding the entire cultures directly to equal volumes of lysis solution and following the subsequent steps described before (64). RNA probes were synthesized in vitro, and RNase T_2 protection assays were performed as described previously (64). Plasmids used as templates to synthesize ^{32}P-labeled RNA probes were linearized with the following enzymes: probes 1, 3, and 4, *Bam*HI; probe 2, *Bst*EII; and probe 5, *Eco*RI. The amounts of total bacterial RNA added to each hybridization reaction were equalized on the basis of A_{260} readings and by comparing the intensities of rRNA bands on agarose gels stained with ethidium bromide (64). Protected regions of probes were analyzed by 7 M urea–5% (wt/vol) polyacrylamide gel electrophoresis (64). Radioactivity in bands on dried gels was measured directly by using an Instant Imager (Packard Instrument Co., Meriden, Conn.).

PCR conditions. The PCR mixture (50 μl) used to synthesize the insert in pTX552 (Table 1) contained 0.5 μg of purified plasmid pTX464 (Table 1), 1× PCR buffer, 1 μM each custom PCR primers *serC* (*pdxF*)-*Eco*RI (5′-GGAATT CAACGGTTTTACTCATTGCG-3′) and *serC* (*pdxF*)-*Bam*HI (5′-TTGGATCC GCAGCAAACTGACCGCGACC-3′), 0.2 mM deoxynucleoside triphosphates, and 1 U of Vent (Exo$^+$) DNA polymerase. The PCR cycle of 94°C for 1 min, 55°C for 1 min, and 72°C for 24 s was carried out 25 times by using a GeneAmp PCR system 2400 (Perkin-Elmer, Norwalk, Conn.).

PCR detection of single or multiple λ prophage was performed as described previously (51) except for the method of cell preparation and that Vent (Exo$^-$) replaced *Taq* DNA polymerase in PCR. Suspected lysogens were grown overnight in LB broth containing kanamycin and streptomycin at 37°C with shaking. Then 0.5 ml of culture was transferred to a microcentrifuge tube, and cells were collected by centrifugation for 1 min at 4°C. The pellet was suspended in 1 ml of cold water, and the cells were collected again by centrifugation. The washing was repeated two more times, and the final pellet was suspended in 1 ml of cold 10 mM Tris-HCl (pH 7.9)–0.1 mM EDTA; 4 μl of the final cell suspension was added to PCR mixtures (51).

Differential rate of β-galactosidase synthesis. Samples were taken for assays from exponentially growing cultures at 37°C starting at turbidities of about 20 Klett (660 nm) units. Total β-galactosidase activity was determined as described previously (41) except that enzyme reaction mixtures were incubated at 30°C instead of 28°C and the A_{415} (*o*-nitrophenyl-β-D-galactopyranoside cleavage) and A_{595} (cell mass) were determined in microtiter plates by a temperature-controlled BT2010 Thermokinetic Reader (Fisher Scientific, Inc.). Readings for microtiter plate wells were converted to corresponding A_{420} and A_{600} values measured by a standard spectrophotometer (1-cm path length) by generating conversion curves containing at least 10 points as described previously (40). Differential rates of β-galactosidase synthesis were determined from plots of total β-galactosidase activity per milliliter of culture (A_{420} per time of reaction [minutes] per volume [milliliters] of cells assayed) versus cell mass (A_{600}) as described previously (59). In some cases, β-galactosidase specific activities were measured in early- or middle-exponential-phase cultures as described previously (41), using the plate reader.

Quantitative Western immunoblotting. Ten-milliliter cultures of *serC* (*pdxF*)-*aroA*$^+$/λ{Φ(*serC* [*pdxF*]′-*lacZYA*)} merodiploid strains TX3187, TX3282, and TX3274 were grown at 37°C in the media indicated to a turbidity of 50 Klett (660 nm) units. *serC* (*pdxF*)::Mu*dI* insertion mutant TX3516 was grown similarly in MMGlu supplemented with 6 mM setine, 0.1 mM tryptophan and L-tyrosine, 0.3 mM phenylalanine, 0.1 mM threonine, and 1 μM pyridoxine, where threonine was added to relieve inhibition of cell growth by serine (22). Cells were collected by centrifugation, and extracts were prepared and boiled for 10 min as described

TABLE 1. *E. coli* K-12 strains and plasmids

Stain or plasmid	Genotype and phenotype[a]	Source or reference
Strains		
GE1050	MC4100 Δ*crp*::Cm^r; Cm^r	G. Weinstock collection
NK7049	Δ*lacX*74 *galOP*308 *rpsL*; Sm^r	R. W. Simons (56)
NU1107	VJS433 *serC*::<mini-Mu*d*I194; Km^r	Laboratory stock (31)
RH74	MC4100 Δ*cya*851 *ilv*::Tn*10*; Tc^r	R. Hengge-Aronis (33)
RO70	MC4100 Φ(*cis-5*::*lacZ*) (λp*lac*Mu55) *lrp-201*::Tn*10*; Tc^r	R. Hengge-Aronis (33)
S90C	*ara* Δ(*lac-pro*) *strA* Sm^r	J. H. Miller (6)
TX3187[b]	NK7049 λ{Φ(*serC* [*pdxF*]′-*lacZYA*)}-478; Sm^r Km^r	λ lysogen with insert from pTX478
TX3274	TX3187 *lrp-201*::Tn*10*; Sm^r Km^r Tc^r	TX3187 × P1*vir*(RO70)
TX3280	TX3187 Δ*cya*851 *ilv*::Tn*10*; Sm^r Km^r Tc^r	TX3187 × P1*vir*(RH74)
TX3282	TX3187 Δ*crp*::Cm^r; Sm^r Km^r Cm^r	TX3187 × P1*vir*(GE1050)
TX3359	TX3187 *lrp-201*::Tn*10* Δ*crp*::Cm^r; Sm^r Km^r Tc^r Cm^r	TX3274 × P1*vir*(GE1050)
TX3516	NK7049 *serC*::<mini-Mu*d*I194; Sm^r Km^r	NK7049 × P1*vir*(NU1107)
TX3728[b]	NK7049 λ[Φ(*serC* (*pdxF*)′-*lacZYA*)]-518; Sm^r Km^r	λ lysogen with insert from pTX518
TX3733[b]	NK7049 λ{Φ(*serC* [*pdxF*]′-*lacZYA*)}-519; Sm^r Km^r	λ lysogen with insert from pTX519
TX3736[b]	NK7049 λ{Φ(*serC* [*pdxF*]′-*lacZYA*)}-520; Sm^r Km^r	λ lysogen with insert from pTX520
TX3773	TX3728 *lrp-201*::Tn*10*; Sm^r Km^r Tc^r	TX3728 × P1*vir*(RO70)
TX3774	TX3733 *lrp-201*::Tn*10*; Sm^r Km^r Tc^r	TX3733 × P1*vir*(RO70)
TX3775	TX3736 *lrp-201*::Tn*10*; Sm^r Km^r Tc^r	TX3736 × P1*vir*(RO70)
TX3782	TX3728 Δ*crp*::Cm^r; Sm^r Km^r Cm^r	TX3728 × P1*vir*(GE1050)
TX3783	TX3733 Δ*crp*::Cm^r; Sm^r Km^r Cm^r	TX3733 × P1*vir*(GE1050)
TX3784	TX3736 Δ*crp*::Cm^r; Sm^r Km^r Cm^r	TX3736 × P1*vir*(GE1050)
TX3815	TX3728 *lrp-201*::Tn*10* Δ*crp*::Cm^r; Sm^r Km^r Tc^r Cm^r	TX3773 × P1*vir*(GE1050)
TX3816	TX3733 *lrp-201*::Tn*10* Δ*crp*::Cm^r; Sm^r Km^r Tc^r Cm^r	TX3774 × P1*vir*(GE1050)
TX3817	TX3736 *lrp-201*::Tn*10* Δ*crp*::Cm^r; Sm^r; Km^r Tc^r Cm^r	TX3775 × P1*vir*(GE1050)
TX3873[b]	NK7049 λ{Φ(*serC* [*pdxF*]′-*lacZYA*)}-552; Sm^r Km^r	λ lysogen with insert from pTX552
TX3875	TX3873 *lrp-201*::Tn*10*; Sm^r Km^r Tc^r	TX3873 × P1*vir*(RO70)
TX3876	TX3873 Δ*crp*::Cm^r; Sm^r Km^r Cm^r	TX3873 × P1*vir*(GE1050)
TX3908	TX3873 *lrp-201*::Tn*10* Δ*crp*::Cm^r; Sm^r Km^r Tc^r Cm^r	TX3876 × P1*vir*(RO70)
Plasmids		
pGEM-3Z	Vector for riboprobe synthesis; Ap^r	Promega Corp.
pNU174	pBR322 containing 4.7-kb *serC*$^+$ *aroA*$^+$ *Hin*dIII-*Sph*I fragment; Ap^r	Laboratory stock (31)
pRS551	Vector for operon fusion construction; Ap^r Km^r	R. W. Simons (56)
pTX463[c]	533-bp *Nde*I-*Kpn*I fragment containing Lrp and CRP boxes and $P_{serC\ (pdxF)}$ from pNU174 cloned into the *Sma*I site of pGEM-3Z; *serC* (*pdxF*)-*aroA* opposite orientation to *lacZ*; Ap^r; source of antisense RNA probe 1	This work
pTX464[c]	Same as pTX463 except *serC* (*pdxF*)-*aroA* same orientation as *lacZ*; Ap^r; source of sense RNA probe 1 and 2	This work
pTX467[c]	839-bp *Bgl*I fragment from pNU174 cloned into *Sma*I site of pGEM-3Z; *serC* (*pdxF*)-*aroA* opposite orientation to *lacZ*; Ap^r; source of antisense RNA probe 3	This work
pTX468[c]	Same as pTX467 except *serC* (*pdxF*)-*aroA* same orientation as *lacZ*; Ap^r; source of sense RNA probe 3	This work
pTX473[c]	345-bp *Ear*I-*Ssp*I fragment from pNU174 cloned into *Sma*I site of pGEM-3Z; *serC* (*pdxF*)-*aroA* opposite orientation to *lacZ*; Ap^r; source of antisense RNA probe 4	This work
pTX474[c]	Same as pTX473, except *serC* (*pdxF*)-*aroA* same orientation as *lacZ*; Ap^r; source of sense RNA probe 4	This work
pTX478	544-bp *Eco*RI-*Bam*HI fragment from pTX463 cloned into the *Eco*RI and *Bam*HI sites of pRS551; Ap^r Km^r	This work
pTX509[c]	456-bp *Bst*EII-*Bam*HI fragment containing Lrp and CRP boxes and $P_{serC\ (pdxF)}$) from pTX463 cloned into *Sma*I site of pGEM-3Z; Ap^r	This work
pTX510[c]	410-bp *Tfi*I-*Bam*HI fragment containing CRP box and $P_{serC\ (pdxF)}$ from pTX463 cloned into *Sma*I site of pGEM-3Z; Ap^r	This work
pTX511[c]	154-bp *Bsr*DI fragment containing $P_{serC\ (pdxF)}$ from pTX463 cloned into *Sma*I site of pGEM-3Z; Ap^r	This work
pTX518	477-bp *Eco*RI-*Bam*HI fragment from pTX509 cloned into *Eco*RI and *Bam*HI sites of pRS551; Ap^r Km^r	This work
pTX519	431-bp *Eco*RI-*Bam*HI fragment from pTX510 cloned into *Eco*RI and *Bam*HI sites of pRS551; Ap^r Km^r	This work
pTX520	175-bp *Eco*RI-*Bam*HI fragment from pTX511 cloned into *Eco*RI and *Bam*HI sites of pRS551; Ap^r Km^r	This work
pTX552	373-bp *Eco*RI-*Bam*HI digested PCR fragment containing $P_{serC\ (pdxF)}$ cloned into *Eco*RI and *Bam*HI sites of pRS551; Ap^r Km^r	This work
pTX576[c]	596-bp *Bst*EII-*Bss*HII fragment from pNU174 cloned into *Sma*I site of pGEM-3Z; *serC* (*pdxF*)-*aroA* same orientation as *lacZ*; Ap^r; source of RNA probe 5	This work

[a] Ap^r, Sm^r, Km^r, Cm^r, and Tc^r, resistance to ampicillin, streptomycin, kanamycin, chloramphenicol, and tetracycline, respectively.
[b] Inserts in λ lysogens are depicted in Fig. 2.
[c] Fragments were filled in or chewed back or both with T4 DNA polymerase before ligation to *Sma*I digested pGEM-3Z.

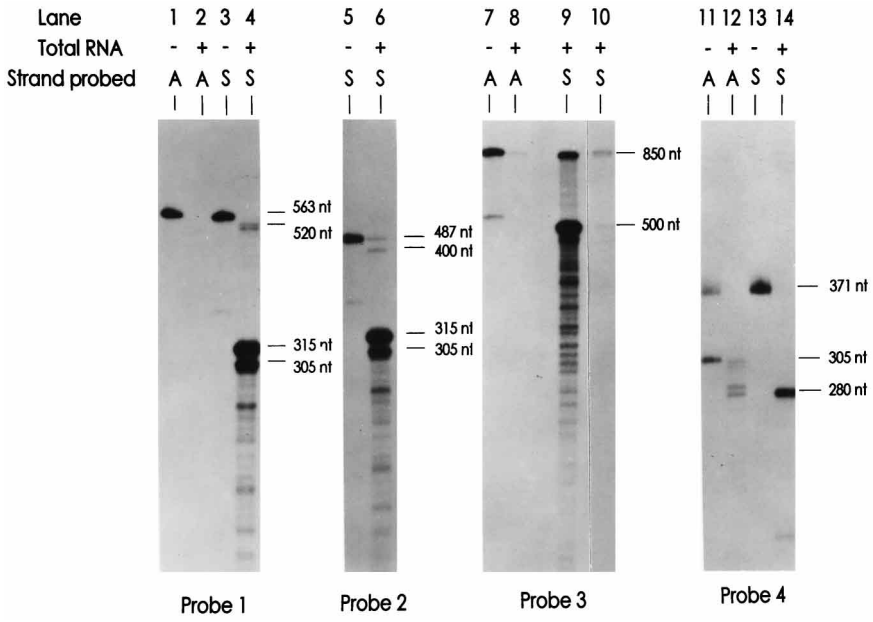

FIG. 3. RNase T_2 protection assays of transcripts synthesized from the *serC* (*pdxF*)-*aroA* region of the *E. coli* K-12 chromosome in *serC* (*pdxF*)$^+$-*aroA*$^+$ parent NK7049 and *serC* (*pdxF*)::<mini-Mu*d*I194 mutant TX3516. NK7049 and TX3516 were grown exponentially with shaking at 37°C in MMGlu and supplemented MMGlu, respectively (Materials and Methods). Ten micrograms of total bacterial RNA (+ above lanes) isolated from NK7049 (lanes 1 to 9 and 11 to 14) and TX3516 (lane 10) was hybridized with ^{32}P-labeled RNA probes 1 to 4 for the sense (mRNA; S) and antisense (transcribed; A) strands (Fig. 2; Materials and Methods). Hybrids were digested with RNase T_2, and protected segments of probes were resolved by urea-polyacrylamide gel electrophoresis (Materials and Methods). Lanes for probe alone lacking total bacterial RNA are marked (−). Sizes of protected bands were determined from standard curves of mobility plotted against the calculated sizes of the full-length probes and other RNA molecular markers (not shown) as described elsewhere (64).

before (29, 70). Protein concentrations of lysates were determined by using the Bio-Rad D*c* micro-Lowry protein assay (Bio-Rad Laboratories, Hercules, Calif.) with bovine serum albumin as the standard. Western immunoblotting of 15% sodium dodecyl sulfate-polyacrylamide gels was performed as described previously (70) except that the blocking solution was 20 mM Tris-HCl (pH 8.2)–0.9% (wt/vol) NaCl–5% (wt/vol) nonfat dry milk. Membranes were incubated with a 1:1,000 dilution of rabbit anti-His_6-SerC (PdxF) antiserum and with a 1:2,000 dilution of goat anti-rabbit immunoglobulin G antiserum conjugated with alkaline phosphatase. The intensities of SerC (PdxF) bands on immunoblots were determined by scanning air-dried polyvinylidene difluoride membranes with a UC630 MaxColor scanner (UMAX Data System Inc., Taiwan). Scanned images of bands were saved into Adobe Photoshop and quantitated by using NIH Image software (version 1.42f).

RESULTS

Transcriptional organization of the *serC* (*pdxF*)-*aroA* operon. We performed RNase T_2 protection assays of transcripts synthesized in vivo from the chromosomal *serC* (*pdxF*)-*aroA* operon of strain NK7049 grown exponentially in MMGlu (Fig. 3; Materials and Methods). RNA probes 1 and 2 shared a common end within *serC* (*pdxF*) but differed in their upstream lengths (Fig. 2). Strong bands corresponding to protected transcripts of 315 and 305 nt were detected with probes 1 and 2 for the *serC* (*pdxF*) sense strand (Fig. 3, lanes 4 and 6). The 305-nt band was not observed in every experiment or with probe 5, which extended further downstream than probe 2 (Fig. 2; see below); therefore, this shorter band represented slight over digestion of duplex RNA by RNase T_2. The 315-nt band placed the in vivo transcription start 58 ± 6 bp upstream from the start codon of the *serC* (*pdxF*) reading frame. Previous S1 nuclease mapping of *serC* (*pdxF*) transcripts from a multicopy plasmid detected a cluster of protected bands, with the longest corresponding to a transcription start 58 bp upstream of the *serC* (*pdxF*) reading frame. Thus, our results confirm this assignment for *serC* (*pdxF*) transcription from the bacterial chromosome. The level of read-through transcription into *serC* (*pdxF*)-*aroA* from upstream (520- and 400-nt bands in Fig. 3, lanes 4 and 6) was minimal (<3%), and no antisense transcription or DNA contamination of our RNA preparations was detected from this region (Fig. 3, lane 2).

Probe 3 spanned the intercistronic region between *serC* (*pdxF*) and *aroA* (Fig. 2). The 850-nt band corresponded to the full-length-protected *serC* (*pdxF*)-*aroA* cotranscript (Fig. 3, lane 9). The prominent 500-nt band corresponded to *serC* (*pdxF*) transcripts that were likely terminated at a strong Rho-independent terminator located 20 to 49 nt downstream and 22 to 51 nt upstream from the end and beginning of the *serC* (*pdxF*) and *aroA* reading frames, respectively (14). However, we cannot rule out the possibility that some of the 500-nt band arose by degradation of the *serC* (*pdxF*)-*aroA* cotranscript back to the stem-loop in the putative terminator. In either case, the amount of the 850-nt full-length band was much lower than that of the 500-nt *serC* (*pdxF*) band in bacteria grown exponentially in MMGlu at 37°C. Thus, SerC (PdxF) transaminase was mainly expressed from a single-gene transcript in bacteria growing under this and other conditions (see below). No antisense transcription was detected in this region (Fig. 3, lane 8). Finally, a *serC* (*pdxF*)::mini-Mu*d*I insertion largely eliminated both the *serC* (*pdxF*) and *serC* (*pdxF*)-*aroA* cotranscript bands (Fig. 3, lane 10), consistent with the requirement of this mutant for serine, pyridoxine, and aromatic compounds (31). The very faint bands present in lane 10 were likely partially digested probe.

serC (*pdxF*)-*aroA* cotranscripts appeared to terminate completely at a Rho-independent terminator located 40 to 71 nt downstream of the *aroA* translation stop codon (Fig. 2; 280 nt band in Fig. 3, lane 14). Therefore, transcription of the *serC* (*pdxF*)-*aroA* operon did not extend downstream into the next putative open reading frame (EO06419 [28]), which has 90% homology to another hypothetical open reading frame in the

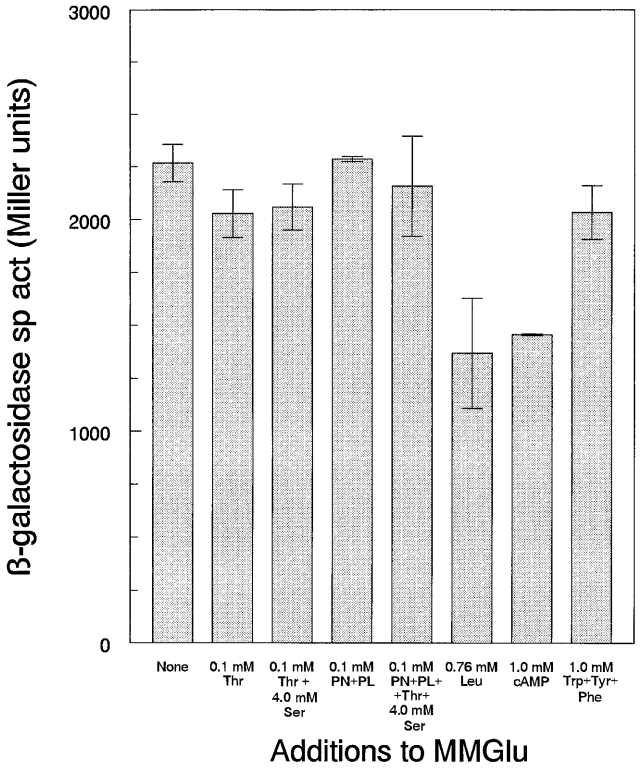

FIG. 4. Expression of the λ{Φ(*serC* [*pdxF*]′-*lacZ*)}-478 operon fusion of strain TX3187 grown exponentially at 37°C in MMGlu supplemented with different compounds. Concentrations of compounds are indicated at the bottom. Threonine was added to prevent inhibition by serine (22). Bacterial cultures were grown to early to middle exponential phase (optical density at 595 nm of 0.24 to 0.45), and β-galactosidase specific activities were determined as described in Materials and Methods. Averages and standard errors of the mean were calculated from at least three independent determinations. PN, pyridoxine; PL, pyridoxal.

speB operon (17). Control hybridization reactions containing tRNA instead of mRNA showed that the apparent antisense transcription into the distal part of *aroA* (280-nt band in Fig. 3, lane 12) was due to conformations assumed by the RNA probe alone (data not shown).

Regulation of *serC* (*pdxF*) transcription. We constructed a λ{Φ(*serC* [*pdxF*]′-*lacZYA*)} operon (transcriptional) fusion extending from 284 bp upstream of the translation start codon of *serC* (*pdxF*) and to 245 bp inside the *serC* (*pdxF*) reading frame (TX3187 [Fig. 1]). The λ{Φ(*serC* [*pdxF*]′-*lacZYA*)} fusion was lysogenized as a single copy into λ*att* of NK7049 (Δ*lac serC* [*pdxF*]$^+$ *aroA*$^+$) (Table 1; Materials and Methods). We first tested whether any of the end products of the pathways mediated by the operon affected *serC* (*pdxF*) transcription levels in cells growing exponentially in MMGlu at 37°C. However, serine, pyridoxine, pyridoxal, or the three aromatic amino acids and three aromatic vitamins had no effect (Fig. 4 and data not shown). We also tested cAMP, because a recent paper reported that transcription of the *serC* (*pdxF*)-*aroA* operon was activated by CRP-cAMP (34). To the contrary, cAMP addition reproducibly reduced *serC* (*pdxF*) transcription instead of stimulating it (Fig. 4). Last, we tested leucine, because Lrp is known to activate the expression of *serA* and other genes involved in one-carbon metabolism (4, 35, 52), and leucine addition reduces *serA* transcription (35, 52). Consistent with this expectation, we found that *serC* (*pdxF*) transcription was reduced by leucine addition (Fig. 4).

These results led to the hypotheses that CRP-cAMP represses and Lrp activates *serC* (*pdxF*)-*aroA* operon transcription. Lrp is at a maximum cellular concentration in bacteria growing exponentially in MMGlu and decreases about 4- to 10-fold in bacteria in amino acid-rich media and LB (4, 32, 44, 45). CRP and cAMP levels are at maximum cellular levels in bacteria growing in media lacking glucose as a carbon source and decrease about 2.5- to 5-fold in bacteria in the presence of glucose (26, 27, 47). Consequently, we determined the differential rates of β-galactosidase synthesis in *crp*$^+$ *lrp*$^+$, *crp*$^+$ *lrp*, *crp lrp*$^+$, and *crp lrp* bacteria growing in different media (Fig. 5 and Table 2). Φ(*serC* [*pdxF*]′-*lacZ*) expression in the *crp*$^+$ *lrp*$^+$ parent strain was maximal in MMGlu and was reduced about 2-, 4-, or 7-fold in MMGly, EMMGlu, or LB, respectively, compared to MMGlu (Fig. 5A; Table 2, column 3). Φ(*serC* [*pdxF*]′-*lacZ*) expression was decreased about twofold in an *lrp* mutant compared to the *lrp*$^+$ parent in MMGlu and remained at the minimum level of expression in *lrp*$^+$ or *lrp* bacteria growing in LB (Fig. 5B; Table 2). A *crp* or *cya* mutation stimulated Φ(*serC* [*pdxF*]′-*lacZ*) expression 2- or 5-fold compared to the *crp*$^+$ parent in bacteria grown in MMGlu or LB, respectively (Fig. 5C; Table 2). Finally, a *crp lrp* double mutant grown in MMGlu or LB had about the same or threefold-higher Φ(*serC* [*pdxF*]′-*lacZ*) expression, respectively, as the *crp*$^+$ *lrp*$^+$ parent. The near equality of Φ(*serC* [*pdxF*]′-*lacZ*) expression in the *crp lrp* and *crp*$^+$ *lrp*$^+$ strains grown in MMGlu is expected if the decrease and increase due to loss of Lrp and CRP-cAMP function, respectively, offset each other.

We confirmed that expression of the Φ(*serC* [*pdxF*]′-*lacZ*) operon fusion reflected normal expression of *serC* (*pdxF*)-*aroA* operon from the bacterial chromosome. The relative amounts of transcript from the normal chromosomal copy of *serC* (*pdxF*)$^+$ in the merodiploid grown in different media were nearly the same as the relative differential rates of β-galactosidase synthesis from the Φ(*serC* [*pdxF*]′-*lacZ*) operon fusion (Table 2, columns 3 and 5; Fig. 6). The relative molar amount of *serC* (*pdxF*) single-gene transcript (≈88% in MMGlu) compared to *serC* (*pdxF*)-*aroA* cotranscript (≈12% in MMGlu) was not strongly regulated by growth in different media (Table 2, column 6; Fig. 6). In fact, the relative amount of *serC* (*pdxF*)-*aroA* cotranscript compared to *serC* (*pdxF*) single-gene transcript may have increased slightly in EMMGlu and LB compared to MMGlu and MMGly (Table 2). Nevertheless, the total amounts of both transcripts were lower in bacteria grown in rich media compared to MMGlu and MMGly (Table 2, columns 3 to 5), and the net effect would still be to decrease both SerC (PdxF) transaminase and AroA synthase amounts in the richer media. Finally, we designed a probe that would allow detection of the $P_{serC\ (pdxF)}$ promoter proximal transcript from both the *serC* (*pdxF*)$^+$ gene and the Φ(*serC* [*pdxF*]′-*lacZ*) operon fusion in the merodiploid strain growing in different media (Fig. 7, lanes 3 to 6). Nearly the same band intensities were observed for *serC* (*pdxF*) transcripts from the chromosome and fusion for each growth condition, and the same patterns of regulation described above were observed for bacteria in the different media. In addition, transcription initiated from the same point upstream of *serC* (*pdxF*) in the chromosomal and fusion copies resulting in a single major protected band (Fig. 7, lanes 3 to 6). Thus, transcription from the Φ(*serC* [*pdxF*]′-*lacZ*) operon fusion reliably reflected that from the bacterial chromosome.

We used quantitative Western immunoblotting to determine whether changes in *serC* (*pdxF*)-*aroA* transcript levels were paralleled by changes in the cellular amount of SerC (PdxF) transaminase (Table 2, column 4; Fig. 8). In these experiments, quantitation standards were prepared by mixing crude extract

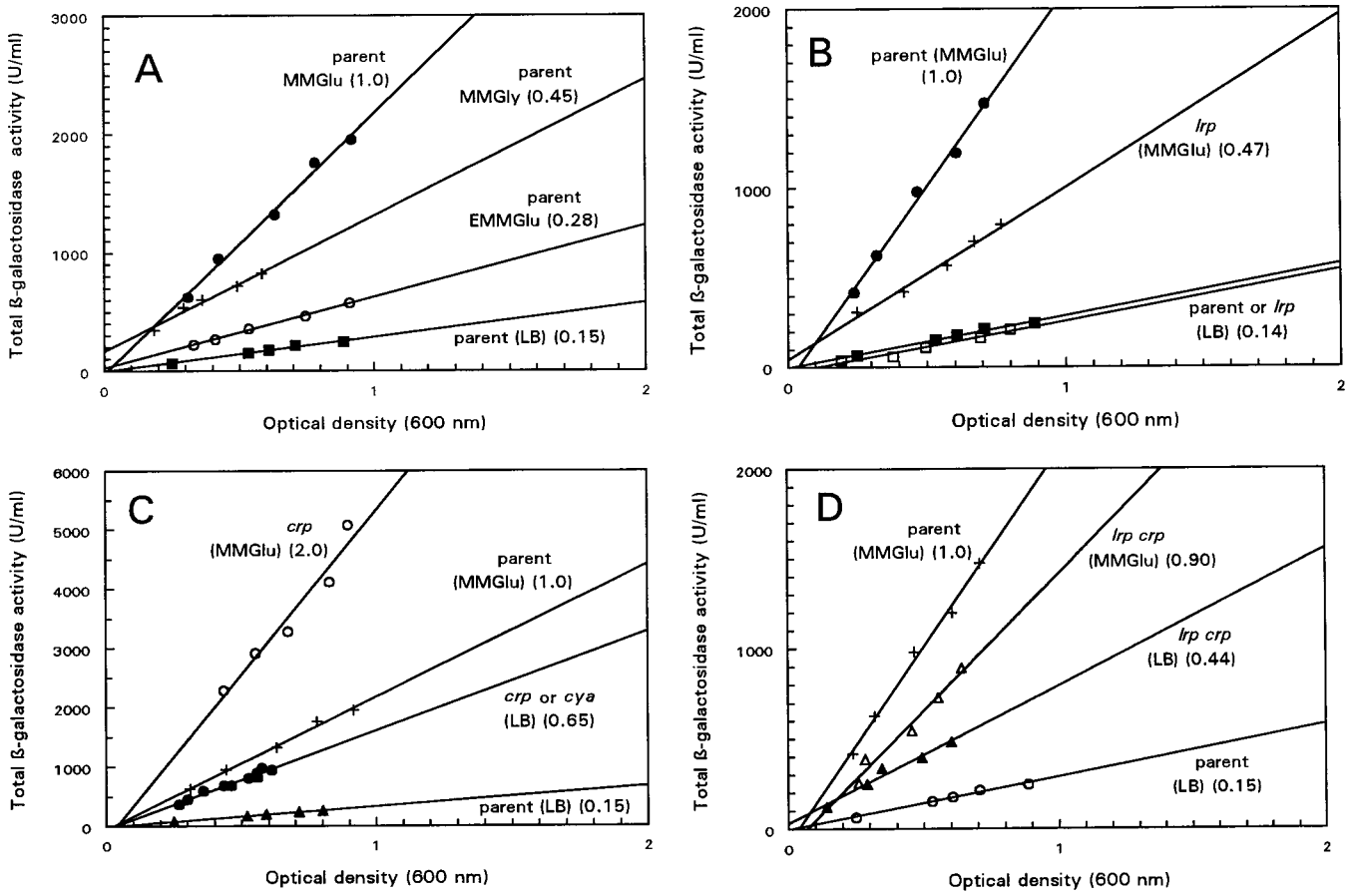

FIG. 5. Representative plots of differential rates of β-galactosidase synthesis from the λ{Φ(*serC* [*pdxF*]′-*lacZ*)}-478 operon fusion in TX3187 (*crp*$^+$ *lrp*$^+$; parent) (A), TX3274 (*crp*$^+$ *lrp*) (B), TX3282 (*crp lrp*$^+$) or TX3280 (*cya lrp*$^+$) (C), and TX3359 (*lrp crp*) (D) (Table 1). The indicated media and β-galactosidase assays are described in Materials and Methods. Lines were fitted by linear regression analysis, and differential rates were calculated from the slopes (Materials and Methods), which were averaged for independent experiments (Table 2). Relative differential rates are given by the numbers in parentheses, where TX3187 expression in MMGlu is set at 1.0.

from a *serC* (*pdxF*) null insertion mutant (Fig. 3, lane 10) with known amounts of purified SerC (PdxF) transaminase (Fig. 8A, lanes 1 to 5; Fig. 8B). The cellular amount of SerC (PdxF) in a crude extract of the *serC* (*pdxF*)-*aroA*$^+$ parent strain run on the same Western blot was then quantitated by comparison to the standards (Materials and Methods). The changes in the relative amounts of SerC (PdxF) transaminase extracted from *crp*$^+$ *lrp*$^+$ cells grown in different media and from *lrp crp*$^+$ and *lrp*$^+$ *crp* mutants paralleled those in *serC* (*pdxF*) transcript amounts and the rates of β-galactosidase synthesis (Table 2, columns 3 to 5). Thus, the regulation of *serC* (*pdxF*) expression occurred at the transcriptional level without any apparent translational control. These experiments allowed us to estimate that SerC (PdxF) was present at about 1,800 dimers per cell (≈5 μM) in bacteria growing exponentially in MMGlu (Table 2; column 4), where each dimer contains two active sites (57).

Sites of regulation by Lrp and CRP-cAMP. The foregoing results strongly supported the hypothesis that Lrp and CRP-cAMP act as positive and negative effectors, respectively, of *serC* (*pdxF*)-*aroA* operon transcription. Examination of the region upstream of the $P_{serC\ (pdxF)}$ promoter revealed a potential Lrp box (CAGTAAAAACATCGG) at positions −141 to −127 relative to the transcription start at +1 (Fig. 2) (14). This putative Lrp box shows 60% matches to the consensus (5) and is positioned appropriately upstream from $P_{serC\ (pdxF)}$ compared with the spacing of known Lrp boxes in other promoters (19). A putative CRP-cAMP binding site (TTGTGTGATGC AAGCCACATTT) is located upstream from $P_{serC\ (pdxF)}$ at positions −99 to −77 (Fig. 2) (34). This possible CRP box shows 64% matches to the consensus (1, 53), but it is situated further upstream from $P_{serC\ (pdxF)}$ than most known CRP boxes are from their promoters (19).

We determined whether these two sites played roles in *serC* (*pdxF*)-*aroA* operon regulation by assaying Φ(*serC* [*pdxF*]′-*lacZ*) fusion expression from a series of mutants containing deletions upstream from $P_{serC\ (pdxF)}$ (Fig. 2). The deletion in strain TX3728 removed DNA to within only 9 bp upstream of the putative Lrp box (Fig. 2). This deletion reduced Φ(*serC* [*pdxF*]′-*lacZ*) expression in bacteria in MMGlu, but not in LB, compared to the starting construct in TX3187 (Table 3, row 1). A small residual decrease in fusion expression was detected in strain TX3728 *lrp* compared to TX3728 *lrp*$^+$ in MMGlu, and there was little difference in the effect of the *crp* and *crp lrp* mutations on expression of the fusions in TX3187 and TX3728. Deletion of the Lrp box in strain TX3733 reduced fusion expression by half compared to TX3187 (Table 3, row 1), and fusion expression in TX3733 was not further reduced in an *lrp* mutant (Table 3, rows 1 and 3). As a control, we tested whether the deletion mutations altered the start points of fusion tran-

TABLE 2. Transcriptional coregulation of *serC* (*pdxF*) and *aroA* in response to growth media and *crp* and *lrp* mutations[a]

Genotype and medium	Growth rate	Differential rate of β-galactosidase synthesis[b]	Amt SerC (PdxF) protein	Total amt of *serC* (*pdxF*) mRNA (10^5)	Molar ratio of *serC* (*pdxF*) to *serC* (*pdxF*)-*aroA* cotranscript
TX3187 *crp*$^+$ *lrp*$^+$ parent					
MMGlu	0.55 ± 0.02 (1.00)	2,207 ± 339 (1.00)	205 ± 32 (1.00)[c]	1.79 ± 0.12 (1.00)[d]	8.4 ± 0.8
MMGly	0.44 ± 0.06 (0.80)	1,002 ± 201 (0.45)	128 ± 9 (0.62)	0.79 ± 0.06 (0.44)	7.7 ± 0.7
EMMGlu	0.97 ± 0.04 (1.8)	624 ± 49 (0.28)	64 ± 8 (0.31)	0.74 ± 0.08 (0.41)	4.5 ± 0.6
LB	1.63 ± 0.06 (3.0)	332 ± 21 (0.15)	24 ± 2 (0.12)	0.35 ± 0.03 (0.20)	5.5 ± 0.7
TX3274 *crp*$^+$ *lrp* mutant					
MMGlu	0.25 ± 0.05 (0.46)	1,028 ± 279 (0.47)	56 ± 14 (0.27)		
LB	1.62 ± 0.08 (3.0)	313 ± 3 (0.14)			
TX3282 *crp lrp*$^+$ mutant					
MMGlu	0.30 ± 0.01 (0.55)	4,461 ± 96 (2.02)			
LB	0.28 ± 0.03 (0.51)	1,434 ± 115 (0.65)	133 ± 15 (0.63)		
TX3280 *cya lrp*$^+$ mutant, LB	0.24 ± 0.01 (0.44)	1,754 ± 165 (0.79)			
TX3359 *crp lrp* mutant					
MMGlu	0.25 ± 0.14 (0.46)	1,990 ± 115 (0.90)			
LB	0.21 ± 0.03 (0.38)	981 ± 65 (0.44)			

[a] Growth rates (doublings per hour), differential rates of β-galactosidase synthesis (β-galactosidase activity per milliliter per cell mass [A_{600}]), amounts of SerC (PdxF) protein (nanograms per 100 μg of crude whole-cell lysate), and RNA amounts (cpm of *serC* [*pdxF*] transcript per genome equivalent) were determined by enzyme assays, quantitative Western immunoblotting, and RNase T_2 protection assays described in Materials and Methods. Experimental errors are expressed as standard (columns 2 to 5) or propagated (column 6) errors of the mean from several independent determinations.

[b] Calculated from slopes in Fig. 5.

[c] Corresponded to 1,800 ± 280 SerC (PdxF) dimers per cell and an intracellular SerC (PdxF) dimer concentration of 4.9 ± 0.8 μM, using 3.3×10^8 cells per ml at 50 Klett (660 nm) units and 100 μg of protein lysate from 8.6×10^8 cells determined here, a molecular mass of SerC (PdxF) dimer of 80 kDa (14), and a volume of cells growing at 0.6 doubling per h of 0.61×10^{-12} ml (11).

[d] Calculated from 12,824 ± 925 and 1,528 ± 148 cpm of total protected *serC* (*pdxF*) mRNA in the single-gene and cotranscript, respectively, per 10 μg of total purified RNA, 20 μg of total RNA per 10^9 cells (3), and 1.6 genome equivalent per cell in bacteria growing at 0.6 doubling per h (3).

scription. We found that the transcription start point for each fusion construct was the same as that from the normal chromosomal copy of *serC* (*pdxF*)-*aroA* (Fig. 7, lanes 8 to 13). These results strongly support the idea that the Lrp box binds Lrp directly as a positive regulator of *serC* (*pdxF*)-*aroA* operon transcription.

Further deletion in strain TX3873 removed both the Lrp and putative CRP boxes (Fig. 2). However, nearly the same relative increase in fusion expression in the *crp* and *crp lrp* mutants was still detected in derivatives of TX3873 as TX3187 grown in MMGlu or LB (Table 3, rows 5 to 8). This result suggested that the putative CRP box does not play a direct role in *serC* (*pdxF*)-*aroA* regulation and that the negative regulatory effects of CRP-cAMP are indirect. Consistent with this interpretation, the fusion in TX3736, which shared the same upstream end as the fusion in TX3873 but ended just 39 bp after the translation start of *serC* (*pdxF*) (Fig. 2), showed the same relative stimulation as all the other strains in response to the *crp* and *crp lrp* mutations. However, the level of *serC* (*pdxF*) expression was reduced in TX3736 derivatives compared to TX3873 derivatives, suggesting that the region between the endpoints of TX3736 and TX3873 may play a role in stabilizing or regulating the amount of *serC* (*pdxF*)-*aroA* transcript produced.

DISCUSSION

We report here that expression of the *serC* (*pdxF*)-*aroA* multifunctional operon is regulated over a 14-fold range by combinations of growth media and regulatory mutations (Fig. 5, 6, 8; Table 2) and a 22-fold range in assays using mutant constructs of the operon (Table 3). This regulation is exerted at the transcriptional level (Fig. 5 and 8; Table 2) and is mediated positively by Lrp (2.2-fold in MMGlu) and negatively by CRP-cAMP (twofold in MMGlu and fivefold in LB) (Fig. 5; Tables 2 and 3). Because the SerC (PdxF) transaminase likely contributes to the control of the flux of intermediates through the serine and PLP biosynthetic pathways, these regulation patterns are physiologically significant. The transcription patterns of the wild-type operon in cells grown in different media and containing *lrp*, *crp*, *cya*, and *lrp crp* mutations can be largely explained in terms of the following model. During growth in

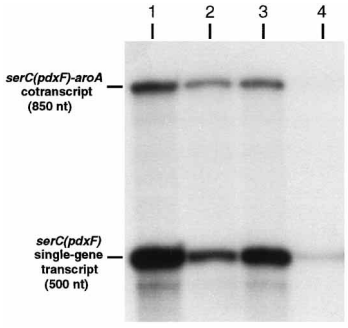

FIG. 6. Amounts of *serC* (*pdxF*) single-gene transcript and *serC* (*pdxF*)-*aroA* cotranscript from the normal chromosomal copy of the *serC* (*pdxF*)$^+$-*aroA*$^+$ operon in fusion strain TX3187 grown exponentially at 37°C in MMG (lane 1), EMMGlu (lane 2), MMGly (lane 3), and LB (lane 4). Bacteria were grown, total bacterial RNA was purified, and RNase T_2 protection assays were performed with RNA probe 3 (Fig. 2 and 3) as described in Materials and Methods. Transcripts from the λ{Φ(*serC* [*pdxF*]′-*lacZ*)}-478 operon fusion in TX3187 were not detected, because the fusion junction in *serC* (*pdxF*) was upstream from the region in probe 3 (Fig. 2). Amounts of transcripts were quantitated as described in Materials and Methods, and molar ratios of *serC* (*pdxF*) single-gene to *serC* (*pdxF*)-*aroA* cotranscript and the counts per minute of *serC* (*pdxF*) single-gene transcript per genome equivalent were calculated (Table 2).

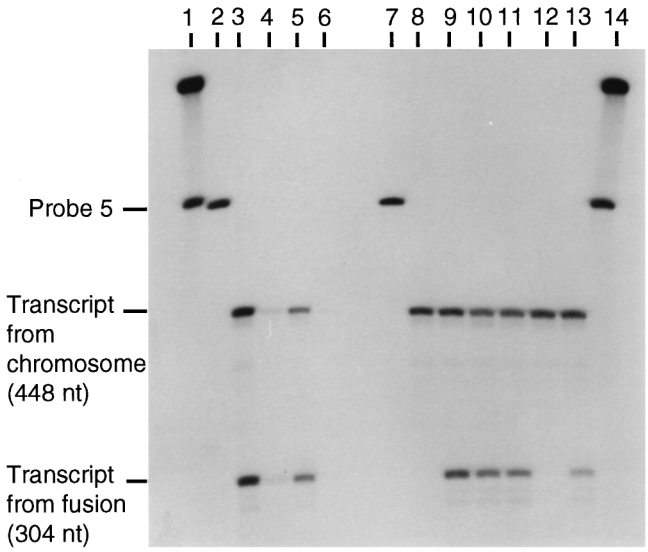

FIG. 7. RNase T_2 protection mapping of the transcription start points from the normal chromosomal copy of *serC* (*pdxF*)$^+$-*aroA*$^+$ and the λ{Φ(*serC* [*pdxF*]′-*lacZ*)} operon fusions in merodiploid strains. Bacteria were grown, total bacterial RNA was purified, and RNase T_2 protection assays were performed with RNA sense-strand probe 5 (Fig. 2) as described in Materials and Methods. Lanes 1 and 14, RNA size markers (upper band, 1,418 nt; lower band, 679 nt); lanes 2 and 7, sense-strand probe 5 alone (649 nt); lanes 3 to 6, protected species from hybridization reactions containing probe 5 and total RNA isolated from TX3187 grown exponentially at 37°C in MMGlu (lane 3), EMMGlu (lane 4), MMGly (lane 5), and LB (lane 6); lanes 8 to 13, protected species from hybridization reactions containing probe 5 and total RNA isolated from the following strains containing different operon fusions (Table 1; Fig. 2) grown exponentially in MMGlu at 37°C: NK7049 control (no operon fusion) (lane 8), TX3187 (fusion-478) (lane 9), TX3728 (fusion-518) (lane 10), TX3733 (fusion-519) (lane 11), TX3736 (fusion-520) (lane 12), and TX3873 (fusion-552) (lane 13). The protected band corresponding to transcription starts from $P_{serC\ (pdxF)}$ in the λ{Φ(*serC* [*pdxF*]′-*lacZ*)}-520 operon fusion in TX3736 (lane 12) was smaller than that of the other strains and was detected at the expected place lower on the gel (data not shown).

MMGlu, cellular Lrp or CRP-cAMP amounts are high or low, respectively (4, 26, 27, 32, 44, 45, 47), which maximizes *serC* (*pdxF*)-*aroA* transcription and SerC (PdxF) transaminase amount. In fact, repression by CRP-cAMP is not at a minimum even in MMGlu, since a *crp* mutation further increased operon expression about twofold compared to the *crp*$^+$ parent (Fig. 5; Table 2). As cellular amounts of Lrp or CRP-cAMP drop or increase, respectively, in minimal salts medium containing glycerol instead of glucose or glucose plus amino acids or in rich LB (4, 26, 27, 32, 44, 45, 47), *serC* (*pdxF*)-*aroA* transcript and SerC (PdxF) transaminase amounts drop to the minimal level detected in LB (Fig. 5 to 8; Table 2). During growth in LB, repression of *serC* (*pdxF*)-*aroA* transcription by CRP-cAMP is maximal and stimulation by Lrp is negligible. Moreover, the activation by Lrp and repression by CRP-cAMP seem to be independent, because the *serC* (*pdxF*) transcription level in the *crp lrp* double mutant was intermediate to those in the *crp* and *lrp* single mutants grown in MMGlu (Table 2).

Maximization of *serC* (*pdxF*)-*aroA* transcription and SerC (PdxF) transaminase amount in cells growing in MMGlu is correlated with the large conversion (as much as 15%) of glucose into serine, which is funneled into glycine, tryptophan, phospholipid, and enterochelin biosynthesis and one-carbon metabolism (Fig. 1) (4, 50). This maximization of SerC (PdxF) protein amount may also ensure a sufficient supply of PLP coenzyme in rapidly metabolizing *E. coli* cells. The antagonism of the Lrp and CRP-cAMP global regulators also provides a mechanism for reduction of *serC* (*pdxF*)-*aroA* transcription and SerC (PdxF) transaminase and AroA synthase amounts in cells growing in amino acid-rich media, which provide serine and decrease the need for B_6 vitamers PLP and pyridoxamine 5′-phosphate.

The combination of Lrp and CRP-cAMP regulation described above likely plays a role in regulating transcription of *serA*, which encodes the dehydrogenase that carries out the first step in serine biosynthesis (Fig. 1). *serA* transcription is positively regulated about fivefold by Lrp (35, 45, 52). Similar to the case for *serC* (*pdxF*)-*aroA* (Fig. 4), *serA* expression was reduced 1.7- to 2.4-fold by leucine addition and about 10-fold when cells were grown in lactate and certain amino acids (39, 58). Unpublished results were consistent with CRP-cAMP repression of *serA* expression, but these analyses were incomplete (39). Taken together, these findings suggest parallel regulation of SerA dehydrogenase and SerC (PdxF) transaminase amounts. It will be interesting to learn whether the expression of other genes involved in serine biosynthesis or one-carbon metabolism are regulated by Lrp activation and CRP-cAMP repression. Other operons regulated by both Lrp and CRP-cAMP include *dad* (degradative D-amino acid dehydrogenase [37]), *daa* (F1845 fimbrial adhesin [2]), and *osmY* (osmotically

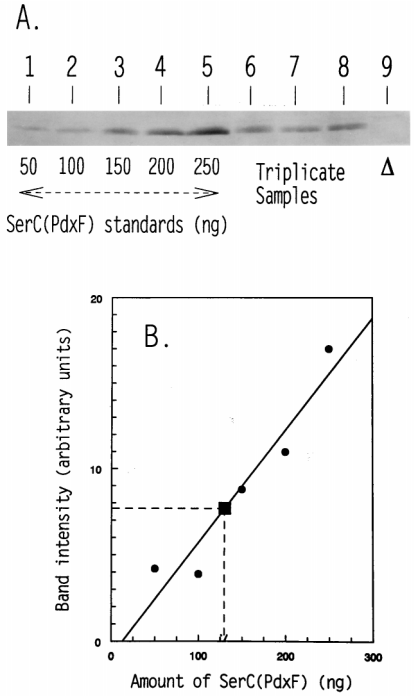

FIG. 8. Representative quantitative Western immunoblot used to determine the cellular amount of SerC (PdxF) transaminase in strain TX3187 grown exponentially in EMMGlu at 37°C. (A) Segment of the immunoblot containing SerC (PdxF) protein. Extracts and blotting were done as described in Materials and Methods. Lanes 1 to 5, standards containing 100 μg of extract from the *serC* (*pdxF*)::Mu*dI* null mutant TX3516 grown in EMMGlu mixed with the indicated amounts of purified native SerC (PdxF) protein; lanes 6 to 8, replicate 100-μg samples of a TX3187 extract; lane 9, 100 μg of extract from TX3516 grown in EMMGlu. (B) ●, standard curve of the intensities of the SerC (PdxF) bands in arbitrary scanner units from panel A plotted against the amount of purified SerC (PdxF) protein added to extracts of TX3516 (A, lanes 1 to 5); ■, SerC (PdxF) amount in the average of the triplicate samples of TX3187 (A, lanes 6 to 8). Immunoblots and quantitation of SerC (PdxF) amounts in TX3187 grown in MMGlu, MMGly, and LB, TX3274 grown in MMGlu, and TX3282 grown in LB were performed similarly (Table 2). In each experiment, extracts used to generate standard curves were prepared from TX3516 grown in the same medium as TX3187.

TABLE 3. Expression of λ{Φ(*serC* [*pdxF*]-*lacZ*)} operon fusions containing deletions upstream of the $P_{serC\ (pdxF)}$ promoter

Additional mutations and growth medium	β-Galactosidase sp act (Miller units)[a] in indicated fusion background[b]				
	TX3187	TX3728	TX3733	TX3873	TX3736
crp$^+$ *lrp*$^+$					
MMGlu	2,049 ± 195 (1.0)	1,297 ± 16 (0.63)	994 ± 133 (0.48)	829 ± 60 (0.40)	487 ± 70 (0.24)
LB	322 ± 49 (0.16)	292 ± 26 (0.14)	235 ± 28 (0.11)	288 ± 51 (0.14)	161 ± 62 (0.08)
crp$^+$ *lrp*					
MMGlu	1,131 ± 219 (0.55)	946 ± 40 (0.46)	931 ± 176 (0.45)	800 ± 58 (0.39)	430 ± 23 (0.21)
LB	277 ± 44 (0.14)	238 ± 33 (0.12)	231 ± 39 (0.11)	232 ± 52 (0.11)	151 ± 47 (0.07)
crp lrp$^+$					
MMGlu	3,688 ± 351 (1.8)	2,625 ± 186 (1.3)	1,722 ± 341 (0.84)	1,594 ± 88 (0.78)	899 ± 74 (0.44)
LB	1,151 ± 86 (0.56)	804 ± 62 (0.39)	886 ± 88 (0.43)	812 ± 117 (0.40)	517 ± 71 (0.25)
crp lrp					
MMGlu	2,026 ± 80 (0.99)	1,908 ± 172 (0.93)	1,886 ± 240 (0.92)	1,397 ± 272 (0.68)	974 ± 160 (0.48)
LB	1,147 ± 165 (0.56)	883 ± 159 (0.43)	906 ± 150 (0.44)	713 ± 126 (0.35)	465 ± 79 (0.23)

[a] Measured as described in Materials and Methods. Experimental errors are expressed as standard errors of the mean for several independent determinations.
[b] Regions of *serC* (*pdxF*) contained in the fusion backgrounds are depicted in Fig. 2. TX3187 and TX3728 contained the putative Lrp and CRP boxes, TX3733 lacked the Lrp box upstream of $P_{serC\ (pdxF)}$ but contained the CRP box, and TX3873 and TX3736 lacked both the upstream Lrp and CRP boxes.

induced periplasmic protein [33]). However, *dad* expression is directly repressed by Lrp and directly activated CRP-cAMP (37), *daa* expression is activated by both Lrp and CRP-cAMP (2), and *osmY* expression is repressed by both Lrp and CRP-cAMP (33).

Our results do not support several conclusions drawn previously. The implication that SerC (PdxF) transaminase levels are constant in cells grown under different conditions is not consistent with our findings (50, 58). The recent claim that *serC* (*pdxF*)-*aroA* transcription is activated by CRP-cAMP is opposite what we observe (34). There are several notable differences between the experimental system used previously and the one used here. Most importantly, previous studies determined *aroA′-lacZ′* gene fusion expression from multicopy plasmid constructs without controls for changes in plasmid copy numbers (34). In our experiments, we determined *serC* (*pdxF*)′-*lacZ*) operon fusion expression from single-copy λ lysogens (Fig. 5; Table 2). We confirmed our conclusions by direct determinations of *serC* (*pdxF*) single-gene and *serC* (*pdxF*)-*aroA* cotranscript amounts (Fig. 6; Table 2) as well as SerC (PdxF) protein amounts (Fig. 8; Table 2). The previous results suggesting that CRP-cAMP activates *serC* (*pdxF*)-*aroA* operon transcription may reflect some combination of changes in plasmid copy numbers, titration of a regulator (see below), or differences in plasmid and chromosome supercoiling.

We also found that *serC* (*pdxF*)-*aroA* cotranscript levels are regulated by Lrp activation and CRP-cAMP repression (Fig. 6; Table 2). To our knowledge, this is the first example of an aromatic biosynthetic gene regulated by Lrp or CRP-cAMP. The grouping of *aroA* in the same operon as *serC* (*pdxF*) is highly suggestive that this regulation may play some physiological role, possibly in coordinating serine, PLP, and aromatic compound biosynthesis (see the introduction). We found that the amount of *serC* (*pdxF*) single-gene transcript was about five- to eightfold greater than that of *serC* (*pdxF*)-*aroA* cotranscript (Fig. 6; Table 2), and we did not detect an *aroA* single-gene transcript by using sensitive mapping methods (Fig. 3). The decrease in *serC* (*pdxF*)-*aroA* cotranscript amount compared to that of the *serC* (*pdxF*) single-gene transcript was most likely caused by attenuation at a Rho-independent terminator between *serC* (*pdxF*) and *aroA* (Fig. 2) (14, 15, 31). This attenuation was not strongly affected by the growth conditions tested so far (Fig. 6; Table 2) and seemed mainly to provide a nearly constant ratio of *aroA* compared to *serC* (*pdxF*) transcript amounts in cells growing in different media.

Consistent with the relatively strong transcription of the *serC* (*pdxF*) gene, SerC (PdxF) transaminase was an abundant protein (≈1,800 dimers, each with two active sites, per cell) in bacteria grown in MMGlu (Table 2) (57). By comparison, full derepression of the *trp* operon in *trpR*$^+$ bacteria leads to the synthesis of about 1,000 molecules of the tryptophan biosynthetic enzymes per cell (42, 43). Recently, it was shown that affinity-tag-purified SerC (PdxF) utilizes 4-phosphohydroxy-L-threonine as a substrate in the back reaction of the PLP biosynthetic pathway (13). This result was consistent with the conclusion of many previous genetic and feeding experiments that SerC (PdxF) transaminase functions in the de novo PLP biosynthetic pathway (9, 10, 31, 67, 68). However, it was premature to conclude that SerC (PdxF) functions sluggishly in the PLP biosynthetic pathway, like the PdxH oxidase (70) and GapB dehydrogenase (67), because the relative kinetics of the SerC (PdxF) transaminase for its three- and four-carbon substrates in the serine and PLP biosynthetic pathways, respectively, remains to be determined.

Finally, we performed a deletion analysis to determine whether Lrp and CRP boxes upstream of the $P_{serC\ (pdxF)}$ (Fig. 2) played roles in regulation of *serC* (*pdxF*)-*aroA* transcription (Fig. 7; Table 3). We found that maximum operon expression in bacteria growing in MMGlu depended on the presence of the upstream Lrp box and that decreased operon expression caused by an *lrp* mutation was lost when the Lrp box was deleted (Results and Table 3). Thus, it seems likely that Lrp regulated *serC* (*pdxF*)-*aroA* transcription by directly binding to the upstream Lrp box. In contrast, the effects of a *crp* mutation on operon expression were still observed when an upstream putative CRP box was deleted (Results; Table 3). This result implies that either CRP-cAMP repressed operon expression by binding elsewhere in the $P_{serC\ (pdxF)}$ promoter region or the CRP-cAMP repression was indirect and involved changes in the amount or activity of a new repressor. The former hypothesis does not seem likely, because there is no region in the $P_{serC\ (pdxF)}$ promoter that even moderately matches half or all of the CRP consensus box (1, 53). However, there is a strong dyad symmetry reminiscent of an operator that overlaps

the −10 box of the $P_{serC\ (pdxF)}$ promoter (Fig. 2) (14, 31). Studies of binding of Lrp and CRP-cAMP to the $P_{serC\ (pdxF)}$ promoter region are currently in progress. In addition, a search for regulatory mutations that increase *serC* (*pdxF*)*′-lacZ* fusion expression in cells on MacConkey-lactose plates is under way. So far, this screen, which has not yet been saturated, has turned up insertions in *crp* and *cya*. This result confirms the above conclusion that CRP-cAMP represses *serC* (*pdxF*)-*aroA* transcription.

ACKNOWLEDGMENTS

We thank Genshi Zhao for purified SerC (PdxF), H.-C. T. Tsui for help with RNase T_2 protection assays and other methods, Regine Hennge-Aronis, Jeffrey Miller, Robert Simons, and George Weinstock for bacterial strains and phage, and Rowena Matthews, Robert Bender, and members of this laboratory for helpful discussions and critical comments.

This work was supported by Public Health Services grant RO1-GM37561 from the National Institute of General Medical Sciences.

REFERENCES

1. **Berg, O. G., and P. H. von Hippel.** 1988. Selection of DNA binding sites by regulatory proteins. II. The binding specificity of cyclic AMP receptor protein to recognition sites. J. Mol. Biol. **200:**709–723.
2. **Bilge, S. S., J. M. J. Apostol, K. J. Fullner, and S. L. Moseley.** 1993. Transcriptional organization of the F1845 fimbrial adhesion determinant of *Escherichia coli*. Mol. Microbiol. **7:**993–1006.
3. **Bremer, H., and P. P. Dennis.** 1996. Modulation of chemical composition and other parameters of the cell by growth rate, p. 1553–1569. *In* F. C. Neidhardt, R. Curtiss III, J. L. Ingraham, E. C. C. Lin, K. B. Low, B. Magasanik, W. S. Reznikoff, M. Riley, M. Schaechter, and H. E. Umbarger (ed.), *Escherichia coli* and *Salmonella*: cellular and molecular biology, 2nd ed., vol. 2. ASM Press, Washington, D.C.
4. **Calvo, J. M., and R. G. Matthews.** 1994. The leucine-responsive regulatory protein, a global regulator of metabolism in *Escherichia coli*. Microbiol. Rev. **58:**466–490.
5. **Cui, Y., Q. Wang, G. D. Stormo, and J. M. Calvo.** 1995. A consensus sequence for binding of Lrp to DNA. J. Bacteriol. **177:**4872–4880.
6. **Cupples, C. G., and J. H. Miller.** 1989. A set of *lacZ* mutations in *Escherichia coli* that allow rapid detection of each of the six base substitutions. Proc. Natl. Acad. Sci. USA **86:**5354–5349.
7. **Davis, R. W., D. Botstein, and J. R. Roth.** 1980. Advanced bacterial genetics. Cold Spring Harbor Laboratory, Cold Spring Harbor, N.Y.
8. **Dempsey, W. B.** 1980. Biosynthesis of control of vitamin B_6 in *Escherichia coli*, p. 93–111. *In* G. P. Tryiates (ed.), Vitamin B_6—metabolism and role in growth. Food and Nutrition Press, Westport, Conn.
9. **Dempsey, W. B.** 1987. Synthesis of pyridoxal phosphate, p. 539–543. *In* F. C. Neidhardt, J. L. Ingraham, K. B. Low, B. Magasanik, M. Schaechter, and H. E. Umbarger (ed.), *Escherichia coli* and *Salmonella typhimurium*: cellular and molecular biology, vol. 1. ASM Press, Washington, D.C.
10. **Dempsey, W. B., and H. Ito.** 1970. Characterization of pyridoxine auxotrophs of *Escherichia coli*: serine and *pdxF* mutants. J. Bacteriol. **104:**658–667.
11. **Donachie, W. D., and A. C. Robinson.** 1987. Cell division: parameter values and the process, p. 1578–1593. *In* F. C. Neidhardt, J. L. Ingraham, K. B. Low, B. Magasanik, M. Schaechter, and H. E. Umbarger (ed.), *Escherichia coli* and *Salmonella typhimurium*: cellular and molecular biology, vol. 2. American Society for Microbiology, Washington, D.C.
12. **Dougan, G., C. E. Hormaeche, and D. J. Maskell.** 1987. Live oral *Salmonella* vaccines: potential use of attenuated strains as carriers of heterologous antigens to the immune system. Parasite Immunol. **9:**151–160.
13. **Drewke, C., M. Klein, D. Clade, A. Arenz, R. Muller, and E. Leistner.** 1996. 4-*O*-Phosphoryl-L-threonine, a substrate of the *pdxC*(*serC*) gene product involved in vitamin B_6 biosynthesis. FEBS Lett. **390:**179–182.
14. **Duncan, K., and J. R. Coggins.** 1986. The *serC-aroA* operon of *Escherichia coli*. A mixed function operon encoding enzymes from two different amino acid biosynthetic pathways. Biochem. J. **234:**49–57.
15. **Duncan, K., A. Lewendon, and J. R. Coggins.** 1986. Evidence for a mixed operon encoding enzymes from two different biosynthetic pathways. Biochem. Soc. Trans. **14:**263–264.
16. **Feng, G., and M. E. Winkler.** 1995. Single-step purifications of His_6-MutH, His_6-MutL and His_6-MutS repair proteins of *Escherichia coli* K-12. BioTechniques **19:**956–965.
17. **Fricke, J., J. Neuhard, R. A. Kelln, and S. Pedersen.** 1995. The *cmk* gene encoding cytidine monophosphate kinase is located in the *rpsA* operon and is required for normal replication rate in *Escherichia coli*. J. Bacteriol. **177:** 517–523.
18. **Gollub, E. G., H. Zalkin, and D. B. Sprinson.** 1967. Correlation of genes and enzymes, and studies on regulation of the aromatic pathway in *Salmonella*. J. Biol. Chem. **242:**5323–5328.
19. **Gralla, J. D., and J. C. Collada-Vides.** 1996. Organization and function of transcription regulatory elements, p. 1232–1245. *In* F. C. Neidhardt, R. Curtiss III, J. L. Ingraham, E. C. C. Lin, K. B. Low, B. Magasanik, W. S. Reznikoff, M. Riley, M. Schaechter, and H. E. Umbarger (ed.), *Escherichia coli* and *Salmonella*: cellular and molecular biology, 2nd ed., vol. 1. ASM Press, Washington, D.C.
20. **Green, J. M., B. P. Nichols, and R. G. Matthews.** 1996. Folate biosynthesis, reduction and polyglutamylation, p. 665–679. *In* F. C. Neidhardt, R. Curtiss III, J. L. Ingraham, E. C. C. Lin, K. B. Low, B. Magasanik, W. S. Reznikoff, M. Riley, M. Schaechter, and H. E. Umbarger (ed.), *Escherichia coli* and *Salmonella*: cellular and molecular biology, 2nd ed., vol. 1. ASM Press, Washington, D.C.
21. **Griffin, H. G., and A. M. Griffin.** 1991. Cloning and DNA sequence analysis of the *serC-aroA* operon from *Salmonella gallinarium*. J. Gen. Microbiol. **137:**113–121.
22. **Hama, H., Y. Sumita, Y. Kakutani, M. Tsuda, and T. Tsuchiya.** 1990. Target of serine inhibition in *Escherichia coli*. Biochem. Biophys. Res. Commun. **168:**1211–1216.
23. **Hill, R. E., K. Himmeldirk, I. A. Kennedy, R. M. Pauloski, B. G. Sayer, E. Wolf, and I. D. Spenser.** 1996. The biogenetic anatomy of vitamin B_6: a ^{13}C NMR investigation of the biosynthesis of pyridoxol in *Escherichia coli*. J. Biol. Chem. **271:**30426–30435.
24. **Hill, R. E., and I. D. Spenser.** 1996. Biosynthesis of vitamin B_6, p. 695–703. *In* F. C. Neidhardt, R. Curtiss III, J. L. Ingraham, E. C. C. Lin, K. B. Low, B. Magasanik, W. S. Reznikoff, M. Riley, M. Schaechter, and H. E. Umbarger (ed.), *Escherichia coli* and *Salmonella*: cellular and molecular biology, 2nd ed., vol. 1. American Society for Microbiology, Washington, D.C.
25. **Hoiseth, S. K., and B. A. D. Stocker.** 1985. Genes *aroA* and *serC* of *Salmonella typhimurium* constitute an operon. J. Bacteriol. **163:**355–361.
26. **Ishizuka, H., A. Hanamura, T. Kunimura, and H. Aiba.** 1993. A lowered concentration of cAMP receptor protein caused by glucose is an important determinant for catabolite repression in *Escherichia coli*. Mol. Microbiol. **10:**341–350.
27. **Kolb, A., S. Busby, H. Buc, S. Garges, and S. Alhya.** 1993. Transcriptional regulation by cAMP and its receptor protein. Annu. Rev. Biochem. **62:**749–795.
28. **Kroeger, M., and R. Wahl.** 1996. Compilation of DNA sequences of *Escherichia coli* K-12 (ECD and ECDC; update, 1995). Nucleic Acids Res. **24:** 29–31.
29. **Laemmli, U. K.** 1970. Cleavage of structural proteins during the assembly of the head of bacteriophage T4. Nature (London) **227:**680–685.
30. **Lam, H. M., E. Tancula, W. B. Dempsey, and M. E. Winkler.** 1992. Suppression of insertions in the complex *pdxJ* operon of *Escherichia coli* K-12 by *lon* and other mutations. J. Bacteriol. **174:**1554–1567.
31. **Lam, H. M., and M. E. Winkler.** 1990. Metabolic relationships between pyridoxine (vitamin B_6) and serine biosynthesis in *Escherichia coli* K-12. J. Bacteriol. **172:**6518–6528.
32. **Landgraf, J. R., J. Wu, and J. M. Calvo.** 1996. Effects of nutrition and growth rate on Lrp levels in *Escherichia coli*. J. Bacteriol. **23:**6930–6936.
33. **Lange, R., M. Barth, and R. Hengge-Aronis.** 1993. Complex transcriptional control of the σ^{38}-dependent stationary-phase-induced and osmotically regulated *osmY* (*csi-5*) gene suggests novel roles for Lrp, cyclic AMP (cAMP) receptor protein-cAMP complex, and integration host factor in the stationary-phase response of *Escherichia coli*. J. Bacteriol. **175:**7910–7917.
34. **Lim, C.-J., W. Hwang, E.-H. Park, and J. A. Fuchs.** 1994. Cyclic AMP-dependent expression of the *Escherichia coli serC-aroA* operon. Biochim. Biophys. Acta **1218:**250–253.
35. **Lin, R., R. D'Ari, and E. B. Newman.** 1990. The leucine regulon of *E. coli* K-12: a mutation in *rblA* alters expression of L-leucine-dependent metabolic operons. J. Bacteriol. **172:**4529–4535.
36. **Man, T. K., G. Zhao, and M. E. Winkler.** 1996. Isolation of a *pdxJ* point mutation that bypasses the requirement for the PdxH oxidase in pyridoxal 5′-phosphate coenzyme biosynthesis in *Escherichia coli* K-12. J. Bacteriol. **178:**2445–2449.
37. **Mathew, E., J. Zhi, and M. Freundlich.** 1996. Lrp is a direct repressor of the *dad* operon in *Escherichia coli*. J. Bacteriol. **178:**7234–7240.
38. **Matthews, R. G.** 1996. One-carbon metabolism, p. 600–611. *In* F. C. Neidhardt, R. Curtiss III, J. L. Ingraham, E. C. C. Lin, K. B. Low, B. Magasanik, W. S. Reznikoff, M. Riley, M. Schaechter, and H. E. Umbarger (ed.), *Escherichia coli* and *Salmonella*: cellular and molecular biology, 2nd ed., vol. 1. ASM Press, Washington, D.C.
39. **Mckitrick, J. C., and L. I. Pizer.** 1980. Regulation of phosphoglycerate dehydrogenase levels and effect on serine synthesis in *Escherichia coli* K-12. J. Bacteriol. **141:**235–245.
40. **Menzel, R.** 1989. A microtiter plate-based system for the semiautomated growth and assay of bacterial cells for β-galactosidase activity. Anal. Biochem. **181:**40–50.
41. **Miller, J. H.** 1992. A short course in bacterial genetics. Cold Spring Harbor Laboratory, Cold Spring Harbor, N.Y.

42. **Morse, D. E., and C. Yanofsky.** 1969. Amber mutants of the *trpR* regulatory gene. J. Mol. Biol. **44:**185–193.
43. **Morse, D. E., and C. Yanofsky.** 1968. The internal low-efficiency promoter of the tryptophan operon of *Escherichia coli*. J. Mol. Biol. **38:**447–451.
44. **Newman, E. B., and R. Lin.** 1995. Leucine-responsive regulatory protein: a global regulator of gene expression in *E. coli*. Annu. Rev. Microbiol. **49:**747–775.
45. **Newman, E. B., R. T. Lin, and R. D'Ari.** 1996. The leucine/Lrp regulon, p. 1513–1525. *In* F. C. Neidhardt, R. Curtiss III, J. L. Ingraham, E. C. C. Lin, K. B. Low, B. Magasanik, W. S. Reznikoff, M. Riley, M. Schaechter, and H. E. Umbarger (ed.), *Escherichia coli* and *Salmonella*: cellular and molecular biology, 2nd ed., vol. 1. ASM Press, Washington, D.C.
46. **O'Gaora, P., D. Maskel, D. Coleman, M. Cafferkey, and G. Dougan.** 1989. Cloning and characterization of the *serC* and *aroA* genes of *Yersinia enterocolitica*, and construction of an *aroA* mutant. Gene **84:**23–30.
47. **Pastan, I., and S. Adhya.** 1976. Cyclic adenosine 5′-monophosphate in *Escherichia coli*. Bacteriol. Rev. **40:**527–551.
48. **Pittard, A. J.** 1996. Biosynthesis of the aromatic amino acids, p. 458–483. *In* F. C. Neidhardt, R. Curtiss III, J. L. Ingraham, E. C. C. Lin, K. B. Low, B. Magasanik, W. S. Reznikoff, M. Riley, M. Schaechter, and H. E. Umbarger (ed.), *Escherichia coli* and *Salmonella*: cellular and molecular biology, 2nd ed., vol. 1. ASM Press, Washington, D.C.
49. **Pizer, L. I.** 1963. The pathway and control of serine biosynthesis in *Escherichia coli*. J. Biol. Chem. **238:**3934–3944.
50. **Pizer, L. I., and M. L. Potochny.** 1964. Nutritional and regulatory aspects of serine metabolism in *Escherichia coli*. J. Bacteriol. **88:**611–619.
51. **Powell, B. S., D. Court, Y. Nakamura, M. P. Rivas, and C. L. Turnbough, Jr.** 1994. Rapid confirmation of single copy lambda prophage integration by PCR. Nucleic Acids Res. **22:**5765–5766.
52. **Rex, J. H., B. D. Aronson, and R. L. Somerville.** 1991. The *tdh* and *serA* operons of *Escherichia coli*: mutational analysis of the regulatory elements of leucine-responsive genes. J. Bacteriol. **173:**5944–5953.
53. **Saier, J., M. H., T. M. Ramseier, and J. Reizer.** 1996. Regulation of carbon utilization, p. 1325–1343. *In* F. C. Neidhardt, R. Curtiss III, J. L. Ingraham, E. C. C. Lin, K. B. Low, B. Magasanik, W. S. Reznikoff, M. Riley, M. Schaechter, and H. E. Umbarger (ed.), *Escherichia coli* and *Salmonella*: cellular and molecular biology, 2nd ed., vol. 1. ASM Press, Washington, D.C.
54. **Sambrook, J., E. F. Fritsch, and T. Maniatis.** 1989. Molecular cloning: a laboratory manual. Cold Spring Harbor Press, Cold Spring Harbor, N.Y.
55. **Silhavy, T. J., M. L. Berman, and L. W. Enquist.** 1984. Experiments with gene fusions. Cold Spring Harbor Laboratory, Cold Spring Harbor, N.Y.
56. **Simons, R. W., F. Houman, and N. Kleckner.** 1987. Improved single and multicopy *lac*-based cloning vectors for protein and operon fusions. Gene **53:**85–96.
57. **Stark, W., J. Kallen, Z. Markovic-Housley, B. Fol, M. Kania, and J. N. Jansonius.** 1991. The three-dimensional structure of phosphoserine aminotransferase from *Escherichia coli*, p. 111–115. *In* T. Fukui, H. Kagamiyama, K. Soda, and H. Wada (ed.), Enzymes dependent on pyridoxal phosphate and other carbonyl compounds as cofactors. Pergamon Press, New York, N.Y.
58. **Stauffer, G. V.** 1996. Biosynthesis of serine, glycine, and one-carbon units, p. 506–513. *In* F. C. Neidhardt, R. Curtiss III, J. L. Ingraham, E. C. C. Lin, K. B. Low, B. Magasanik, W. S. Reznikoff, M. Riley, M. Schaechter, and H. E. Umbarger (ed.), *Escherichia coli* and *Salmonella*: cellular and molecular biology, 2nd ed., vol. 1. ASM Press, Washington, D.C.
59. **Stewart, V., and C. Yanofsky.** 1986. Role of leader peptide synthesis in tryptophanase operon expression in *Escherichia coli* K-12. J. Bacteriol. **167:**383–386.
60. **Stocker, B. A., S. K. Hoiseth, and B. P. Smith.** 1983. Aromatic-dependent "*Salmonella* sp." as live vaccine in mice and calves. Dev. Biol. Stand. **53:**47–54.
61. **Sugimoto, E., and L. I. Pizer.** 1968. The mechanism of end product inhibition of serine biosynthesis. I. Purification and kinetics of phosphoglycerate dehydrogenase. J. Biol. Chem. **243:**2081–2089.
62. **Sugimoto, E., and L. I. Pizer.** 1968. The mechanism of end product inhibition of serine biosynthesis. II. Optical studies of phosphoglycerate dehydrogenase. J. Biol. Chem. **243:**2090–2098.
63. **Tribe, D. E., H. Camakaris, and J. Pittard.** 1976. Constitutive and repressible enzymes of the common pathway of aromatic biosynthesis in *Escherichia coli* K-12: regulation of enzyme synthesis at different growth rates. J. Bacteriol. **127:**1085–1097.
64. **Tsui, H.-C., A. J. Pease, T. Koehler, and M. E. Winkler.** 1994. Detection and quantitation of RNA transcribed from bacterial chromosomes, p. 179–204. *In* K. Adolph (ed.), Methods in molecular genetics: molecular microbiology. Academic Press, New York, N.Y.
65. **Yang, Y., G. Zhao, and M. E. Winkler.** 1996. Identification of the *pdxK* gene that encodes pyridoxine (vitamin B_6) kinase in *Escherichia coli* K-12. FEMS Microbiol. Lett. **141:**89–95.
66. **Zhao, G.** 1997. Unpublished method.
67. **Zhao, G., A. J. Pease, N. Bharani, and M. E. Winkler.** 1995. Biochemical characterization of *gapB*-encoded erythrose 4-phosphate dehydrogenase of *Escherichia coli* K-12 and its possible role in pyridoxal 5′-phosphate biosynthesis. J. Bacteriol. **177:**2804–2812.
68. **Zhao, G., and M. E. Winkler.** 1996. 4-Phospho-hydroxy-L-threonine is an obligatory intermediate in pyridoxal 5′-phosphate coenzyme biosynthesis in *Escherichia coli* K-12. FEMS Microbiol. Lett. **135:**275–280.
69. **Zhao, G., and M. E. Winkler.** 1994. An *Escherichia coli* K-12 *tktA tktB* mutant deficient in transketolase activity requires pyridoxine (vitamin B_6) as well as the aromatic amino acids and vitamins for growth. J. Bacteriol. **176:**6134–6138.
70. **Zhao, G., and M. E. Winkler.** 1995. Kinetic limitation and cellular amount of pyridoxine (pyridoxamine) 5′-phosphate oxidase of *Escherichia coli* K-12. J. Bacteriol. **177:**883–891.
71. **Zhao, G., and M. E. Winkler.** 1996. A novel alpha-ketoglutarate reductase activity of the *serA*-encoded 3-phosphoglycerate dehydrogenase of *Escherichia coli* K-12 and its possible implications for human 2-hydroxyglutaric aciduria. J. Bacteriol. **178:**232–239.